Article

J. Biol. Regul. Homeost. Agents. 2024; 38(6): 5205–5215
https://doi.org/10.23812/j.biol.regul.homeost.agents.20243806.416

CDC25A Promotes Early Metastasis of Lung Adenocarcinoma through Cell Cycle Regulation

Bin Li[1,*], Xuesong Zhao[1], Haifeng Hu[2], Tianyu Zhang[2], Yi Qi[3], Bo Liu[4], Bing Lan[5]

[1]Department of Laboratory Medicine, The Second Affiliated Hospital of Qiqihar Medical College, 161006 Qiqihar, Heilongjiang, China
[2]Department of Imaging, The Second Affiliated Hospital of Qiqihar Medical College, 161006 Qiqihar, Heilongjiang, China
[3]Department of General Medicine, The First Affiliated Hospital of Qiqihar Medical College, 161042 Qiqihar, Heilongjiang, China
[4]Department of Government Office, The Second Affiliated Hospital of Qiqihar Medical College, 161006 Qiqihar, Heilongjiang, China
[5]Department of Respiratory Medicine, The Second Affiliated Hospital of Qiqihar Medical College, 161006 Qiqihar, Heilongjiang, China
*Correspondence: LIBIN666@qmu.edu.cn (Bin Li)
Submitted: 29 February 2024 Revised: 1 April 2024 Accepted: 12 April 2024 Published: 1 June 2024

Background: Lung adenocarcinoma (LUAD), a malignant tumor, poses a significant threat to human life, with easy metastasis being the primary reason for its low survival rate. Therefore, this study aimed to identify specific biomarkers and molecular mechanisms underlying early metastasis, providing a solid foundation for developing novel LUAD therapies.
Methods: The potential modules associated with LUAD metastasis were analyzed through weighted gene co-expression network analysis, and genes in the key modules were used for functional enrichment. Differentially expressed genes between metastatic and non-metastatic LUAD patients were analyzed using the "limma" package. Blood samples were collected to analyze and validate the expression of target genes. Functional assays were performed to investigate the impacts of cell division cycle 25 A (*CDC25A*) knockdown on cancer cell proliferation, migration, and cell cycle progression.
Results: *CDC25A* was upregulated in LUAD metastasis, and its overexpression was associated with poorer survival. *CDC25A* was significantly overexpressed in patients with LUAD metastasis ($p < 0.0001$). Furthermore, *CDC25A* knockdown inhibited LUAD cell proliferation ($p < 0.01$), migration ($p < 0.0001$), and invasion ($p < 0.0001$), as well as induced G1 cell cycle arrest. Additionally, suppressing *CDC25A* expression significantly reduced the expression of *cyclin D1* ($p < 0.001$), cyclin-dependent kinase 4 (*CDK4*) ($p < 0.001$), and cyclin-dependent kinase 6 (*CDK6*) ($p < 0.0001$).
Conclusion: Our findings demonstrate that *CDC25A* enhances early LUAD metastasis by promoting cell cycle progression. Therefore, targeting *CDC25A* could be a potential therapeutic approach to suppress metastasis in LUAD patients.

Keywords: lung adenocarcinoma; module; secreted protein; prognosis; cell cycle

Introduction

Lung cancer has a high mortality rate globally. Histologically, lung cancer is classified into two main types: small cell carcinoma and non-small cell carcinoma (NSCLC), with NSCLC accounting for approximately 85% of the cases [1]. Lung adenocarcinoma (LUAD), the most prevalent subtype among NSCLC, is primarily treated through immunotherapy, radiation therapy, and non-invasive surgery [2]. Despite considerable advancements in treatment strategies, the prognosis of LUAD remains poor, with a 5-year survival rate of only 18% [3]. Research has suggested that the consequences of LUAD are closely associated with cancer stages at the time of diagnosis. Early-stage LUAD can be effectively treated through surgical resection, improving the 5-year survival rate ranging from 70 to 90% [4]. However, most patients are usually diagnosed at advanced stages, often with metastases, leading to a 1-year survival of only 15–19% [5]. Therefore, elucidating the molecular mechanisms underlying LUAD metastasis is crucial for early-stage diagnosis and developing advanced therapeutic strategies.

Cancer, characterized by uncontrolled cell proliferation, originates from disruption in the cell cycle [6]. Cyclin-dependent kinases (CDKs), a crucial regulatory component of this signaling network, regulate the progression through the cell cycle [7]. CDKs promote cell cycle advancement by phosphorylating and inhibiting the retinoblastoma proteins, inhibiting their activity during cell cycle progression [8]. On the other hand, the phosphatases known as cell division cycle 25 (CDC25) activate CDKs by dephosphorylating them, facilitating cell cycle progression [9]. Among the three CDC25 variants, cell division cycle 25 A (*CDC25A*) is known for its oncogenic properties across multiple cancer types [10]. Accumulating evidence indicates *CDC25A* as an oncogene. *CDC25A* is overexpressed in 50% of breast cancers, correlating with unfavorable outcome [11]. Another study has suggested that the downregulation of *CDC25A* reduces the survival rate and promotes apoptosis in cervical cancer [12]. Additionally, silencing *CDC25A*

Journal of
BIOLOGICAL REGULATORS
and Homeostatic Agents

in nasopharyngeal carcinoma results in cell cycle arrest at the G1 phase and inhibits proliferation [13]. Furthermore, overexpression of *CDC25A* has been associated with poor prognosis in NSCLC [14]. However, its potential role in LUAD metastasis remains unexplored.

Therefore, this study aims to explore the link between the *CDC25A* expression profile and LUAD metastasis. Additionally, it intends to investigate the role of *CDC25A* in LUAD cell invasion and proliferation *in vitro*. Furthermore, this study will provide a solid foundation for considering *CDC25A* as a potential biomarker, offering insights into prognosis and identifying significant therapeutic targets in LUAD.

Materials and Methods

Data and Sample Sources

The mRNA expression matrix for LUAD was obtained from The Cancer Genome Atlas (TCGA) database (https://portal.gdc.cancer.gov/), while the list of secreted proteins was retrieved from The Human Protein Atlas (HPA) (https://www.proteinatlas.org/). Blood samples were collected from 50 early-stage LUAD patients and 50 healthy controls at the Second Affiliated Hospital of Qiqihar Medical College, China. The blood samples were centrifuged at 1500 r/min at 4 °C for 10 minutes. The serum fraction was isolated and stored at –80 °C for further analyses. The study was approved by the Ethical Research Association of the Second Affiliated Hospital of Qiqihar Medical University, China, with the ethical number [2021]1215-1. All the study participants provided informed consent, and the study design adhered to the guidelines outlined in the Declaration of Helsinki.

Weighted Gene Co-Expression Network Analysis (WGCNA)

The "WGCNA" package (version: 1.72-5, https://cran.r-project.org/web/packages/WGCNA/index.html) within the R software environment was utilized to identify the modules of co-expressed genes associated with tumor node metastasis (TNM) stage and metastasis in early-stage LUAD. To establish a weighted adjacency matrix, Pearson correlation coefficients were calculated for all gene pairs using the formula as follows: aij = 0.5× (1 + cor (i, j))^β. Modules related to LUAD metastasis were identified by average hierarchical clustering and thresholding based on connectivity patterns.

Functional Enrichment Analysis

The genes within the modules of interest underwent additional analysis utilizing Gene Ontology (GO, http://geneontology.org/) and the Kyoto Encyclopedia of Genes and Genomes (KEGG, https://www.genome.jp/kegg/) for pathway enrichment. GO analysis aimed to identify enriched biological processes, while KEGG analysis determined overrepresented signaling pathways and cellular functions.

Key Gene Analysis

Differential gene expression analysis between patients with metastatic and non-metastatic LUAD was performed using the "limma" package (version: 3.56.2, https://bioinf.wehi.edu.au/limma/) in R software. Heatmaps were generated utilizing the "pheatmap" package (version: 1.0.12, https://cran.r-project.org/web/packages/pheatmap/index.html). Venn diagrams were drawn to detect and visualize overlaps among various datasets obtained from differentially expressed genes, secreted proteins, and key module genes. Additionally, gene expression boxplots were generated using "ggplot2" (version: 3.4.4, https://ggplot2.tidyverse.org), comparing data obtained from metastatic and non-metastatic groups. All the samples were divided into high expression and low expression groups based on median key gene levels. Survival curves were plotted using the "survival" package (version 3.5-5, https://github.com/therneau/survival) in R software, incorporating both overall and disease-free survival data from TCGA.

Enzyme-Linked Immunosorbent Assay (ELISA)

Out of the total collected serum samples, 30 patients with early-stage LUAD and 30 healthy controls were randomly selected for further analyses. The protein expression levels of target genes were determined using enzyme-linked immunosorbent assay (ELISA) (JL52470, Jianglai Biological, Shanghai, China). However, to compare target gene levels, 15 metastatic and 15 non-metastatic early stage patients were analyzed through ELISA. The optical density (OD) value was assessed at 450 nm using an enzyme maker, VARIOKSKAN LUX (VLBLATGD2, Thermo Fisher Scientific, Waltham, MA, USA).

Cell Culture

The LUAD cell lines such as SPC-A1, XY-XB-1057, and GLC-82, XY-XB-1754, were obtained from the American Type Culture Collection (Shanghai Xuanya Biotechnology, Shanghai, China). The cells were authenticated using short tandem repeat (STR) analysis and were found to be free of cross-contamination using mycoplasma testing. The cells were then maintained in RPMI-1640 medium (R5158, Sigma-Aldrich, Shanghai, China) supplemented with 10% fetal bovine serum (FBS) (12103C, Sigma-Aldrich, Shanghai, China) and antibiotics followed by incubation at 37 °C and 5% CO_2.

Cell Transfection

SPC-A1 and GLC-82 cells were inoculated into a cell culture plate at a density of 1×10^5 cells/well and were al-

lowed to grow until reaching 80% confluence. Transfection was performed employing the Lipofectamine 2000 reagent (11668, Invitrogen, Carlsbad, CA, USA) following the instructions provided with the reagent. The cells were then incubated at room temperature for 5 minutes. The short hairpin RNA targeting CDC25A (sh-CDC25A), the negative control shRNA, and liposome complexes were added to the cells and were allowed to incubate at 37 °C and 5% CO_2 for 48 hours. The sequence of sh-CDC25A used for transfection was 5′-AAGGAAAATGAAGCCTTTGAG-3′. The sh-CDC25A and negative control shRNA were procured from Beyotime Company (L18040 and R7016m, Beyotime Biotechnology, Shanghai, China).

Western Blot Analysis

Total cellular protein was extracted by Radio Immunoprecipitation Assay (RIPA) lysis buffer and was quantified utilizing a BCA assay kit (P00125, Beyotime Biotechnology, Shanghai, China). The quantified proteins were separated through 12% SDS-PAGE and then transferred to the PVDF membrane. The blots were incubated overnight with primary antibodies such as rabbit anti-CDC25A (1:2000, ab989, Abcam, Shanghai, China) and anti-glyceraldehyde-3-phosphate dehydrogenase (GAPDH) (1:2500, ab9485, Abcam, Shanghai, China) at 4 °C. The blots were incubated with the secondary goat anti-rabbit antibody (1:10000, ab175781, Abcam, Shanghai, China) at room temperature for 1 hour. Finally, the blots were prepared and visualized using a chemiluminescence ECL reagent (WBKLS0500, Millipore, Boston, MA, USA). The images of the protein bands were captured using a ChemiDoc XRS+ (1708265, Bio-Rad Laboratories, Hercules, CA, USA) imaging system. Relative concentrations of target proteins were determined using Image-Pro Plus software (5.0.2, Media Cybernetics, Rockville Pike, MD, USA).

CCK-8 Assay

SPC-A1 and GLC-82 cells, transfected with sh-CDC25A or negative control sh-RNA, were seeded at a density of 1×10^5 cells/well and were treated with Cell Counting Kit-8 (CCK-8) reagent (KGA9305, Keygen Biotechnology, Nanjing, China) for 2 hours. The OD was measured at 450 nm using a spectrophotometer (V-5000, Shanghai Metash Instruments, Shanghai, China).

Scratch Assay

SPC-A1 and GLC-82 cells were seeded at a density of 1×10^5 cells/well and were transfected with sh-CDC25A or negative control sh-RNA. Upon reaching 90–100% confluence, scratches were created in each well using a 10 μL sterile pipette tip, marking it as a 0-hour timepoint. After washing with buffer, the cells were cultured in a serum-free medium (RPMI-1640) (R5158, Sigma-Aldrich, Shanghai, China) for 48 hours. Finally, the healing of scratches was visualized using microscopy (CX33, Olympus Corporation, Tokyo, Japan). Migration distance analyzed through Image-Pro Plus software (5.0.2, Media Cybernetics, Rockville Pike, MD, USA).

Transwell Test

SPC-A1 and GLC-82 cells were transfected with sh-CDC25A or negative control sh-RNA and cultured at a density of 1×10^5 (200 μL) in a serum-free medium. The upper chamber of the Transwell inserts was coated with Matrigel matrix (356230, BeiJing Biocreative Technology, Beijing, China) and subsequently filled with the cells along with 200 μL of RPMI-1640 medium without FBS. In contrast, the lower chamber was filled with 500 μL of RPMI-1640 (R5158, Sigma-Aldrich, Shanghai, China) supplemented with 10% FBS (12103C, Sigma-Aldrich, Shanghai, China). After 24 hours of incubation, the migrated cells were fixed and stained with 0.1% crystal violet solution for 20 minutes. Finally, the images were captured, and the number of invaded cells was calculated using a light microscope (magnification, ×200; CX33, Olympus Corporation, Tokyo, Japan).

Flow Cytometry

SPC-A1 cells (1×10^5 cells/well) were seeded in a 6-well plate and transfected with sh-CDC25A or negative control sh-RNA. The cells were harvested after 24 hours of transfection and underwent cell cycle analysis using a cell cycle assay kit (559619, BD Biosciences, New York, NJ, USA) following the manufacturer's instructions. The harvested cells were centrifuged at 1000 ×g for 5 minutes and washed with phosphate balanced solution (PBS). The cells were fixed by adding 500 μL of 70% ethanol and incubating at 4 °C for 1 hour. After washing the cells with PBS, 1 mL of staining solution was added, followed by incubation at room temperature for 30 minutes. Finally, the cells were analyzed using FACSCalibur flow cytometry (342973, BD Biosciences, New York, NJ, USA), and the results were interpreted using ModFit software (version 3.2, Verity Software House, Mountain View, CA, USA).

Real-Time Quantitative PCR (qPCR)

Total RNA was isolated from the cells using TRIzol reagent (15589226, Sigma-Aldrich, Shanghai, China) and converted into cDNA utilizing the microRNA first strand synthesis kit (638313, Takara, Dalian, China). The CellAmp Direct RNA Prep kit (3732, Takara, Dalian, China) was used, adhering to the manufacturer's instructions, to extract and quantify the RNA from the cell for real-time quantitative PCR (qPCR) to determine the expression of *CDC25A*. The relative expression levels were assessed using the $2^{-\Delta\Delta Ct}$ method. All the primers used in the qPCR were synthesized by Takara (Table 1). Each experiment was replicated three times to ensure accuracy.

Journal of
BIOLOGICAL REGULATORS
and Homeostatic Agents

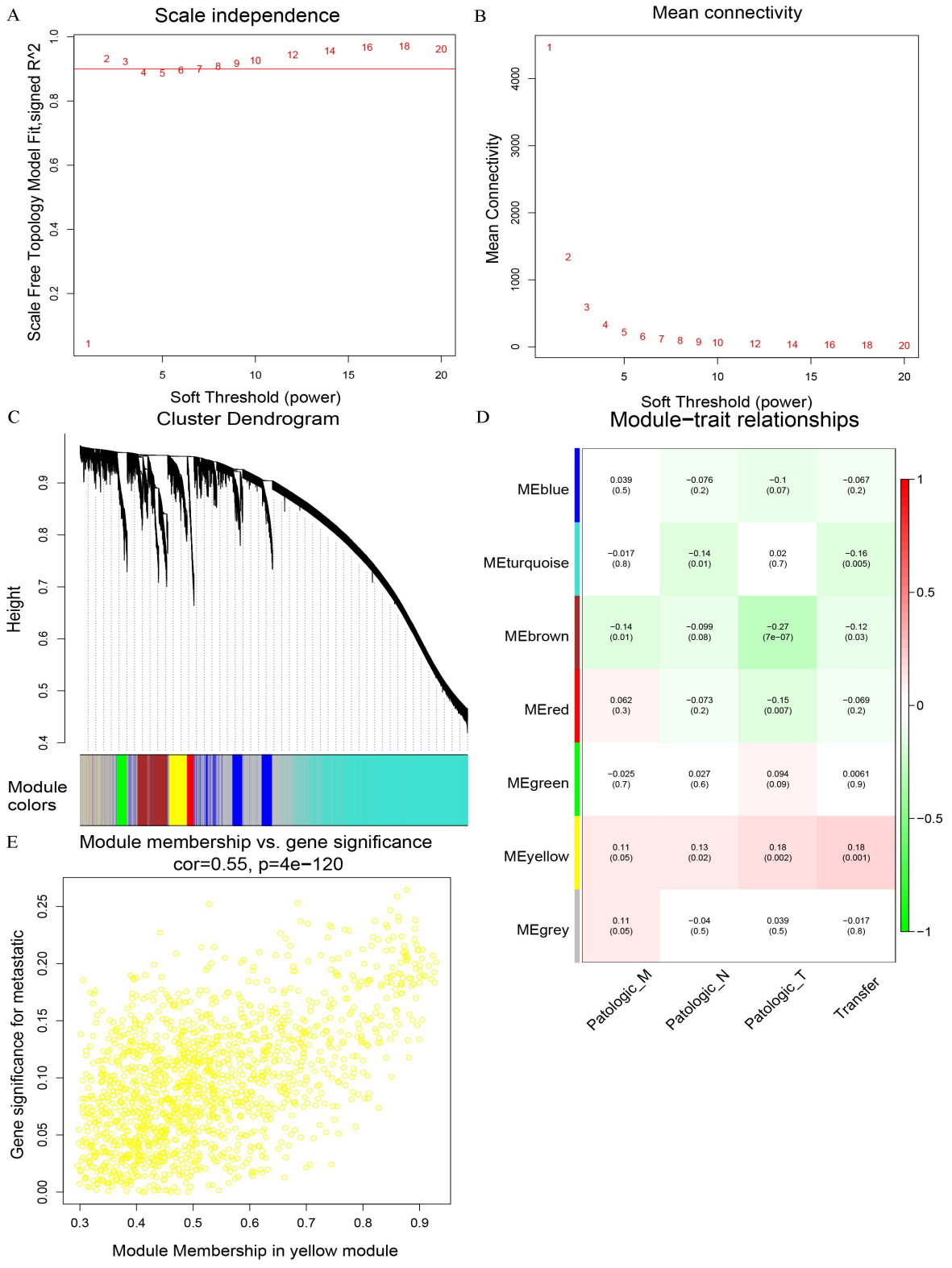

Fig. 1. Identification of key co-expression modules associated with early metastasis in lung adenocarcinoma (LUAD) by weighted gene co-expression network analysis. (A) Scale-free topology model fit analysis of soft-thresholding powers. (B) Mean connectivity analysis of various soft-thresholding powers. (C) Dendrogram of gene hierarchical clustering indicating distinct co-expression modules labeled by color. (D) Heatmap depicting the connection between module eigengenes and clinical features of LUAD. (E) Scatterplot of module membership versus gene significance for the yellow module.

Table 1. A list of primers used in qPCR.

Gene	Forward (5′-3′)	Reverse (5′-3′)
CDC25A	GTGAAGGCTATTGGCG	GGTCATAGTGGACGGTCAGGT
GAPDH	ACCACAGTCCATGCCATCAC	ACCACAGTCCATGCCATCAC-3
Cyclin D1	TCAAGTGTGACCCGGACTG	GCTTCTTCCTCCACTTCCCC
CDK4	GATGCGCCAGTTTCTAAGCG	GGCCAGCTTAACTGTCCCAT
CDK6	CGTGGAAGTTCAGACGTGGA	AAAGCCTGTCTGGGAAGAGC

CDC25A, cell division cycle 25 A; *GAPDH*, glyceraldehyde-3-phosphate dehydrogenase; *CDK*, cyclin-dependent kinase.

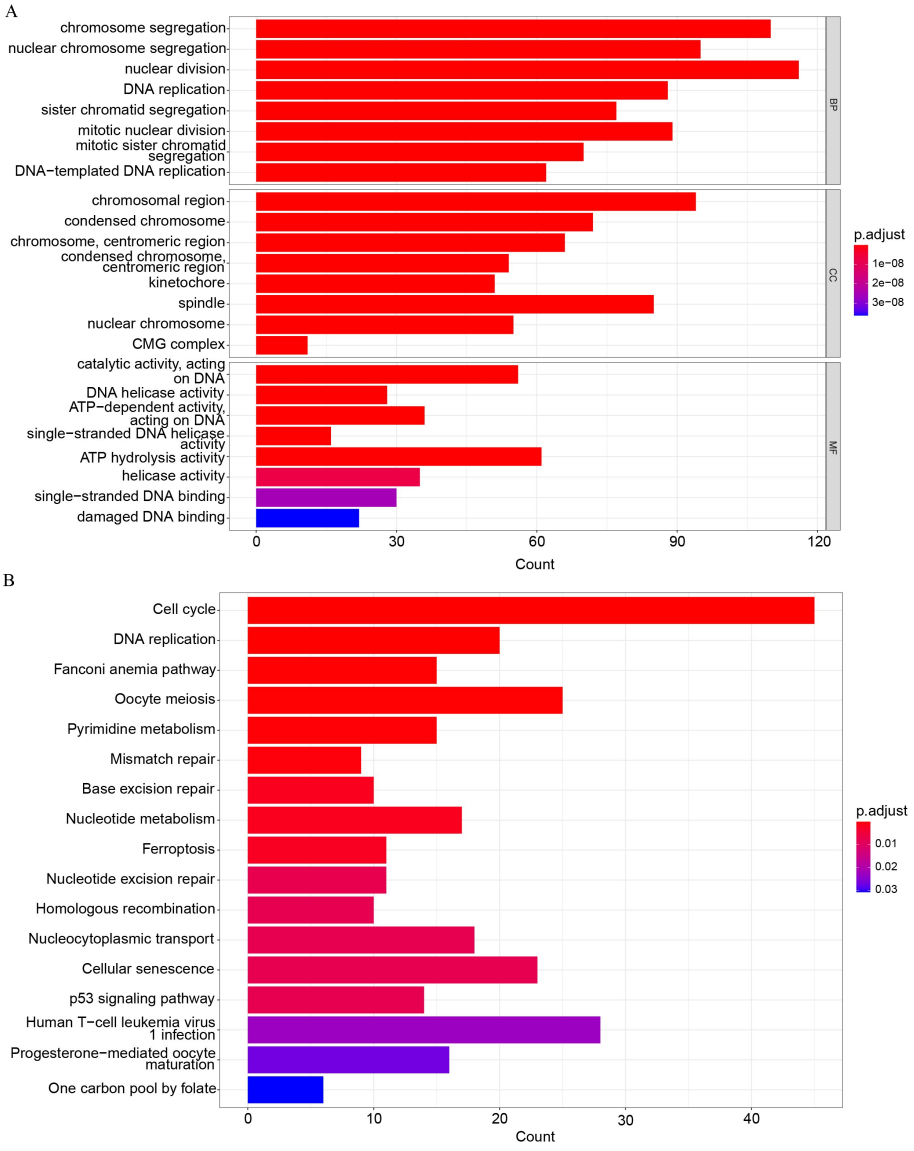

Fig. 2. Functional enrichment analysis of the gene cluster in the yellow module. (A) Gene Ontology (GO) enrichment analysis. (B) Kyoto Encyclopedia of Genes and Genomes (KEGG) pathway analysis. ATP, adenosine triphosphate.

Statistical Analysis

Survival analysis for comparing survival curves was performed using log-rank tests. The experimental data were statistically analyzed using IBM SPSS Statistics 20 software (IBM Corp., Armonk, NY, USA). The comparisons between experimental groups were examined using student's *t*-test or ANOVA, followed by the LSD or Tukey test. A p-value < 0.05 was considered statistically significant ($^{*}p < 0.05$, $^{**}p < 0.01$, $^{***}p < 0.001$, $^{****}p < 0.0001$).

Journal of
BIOLOGICAL REGULATORS
and Homeostatic Agents

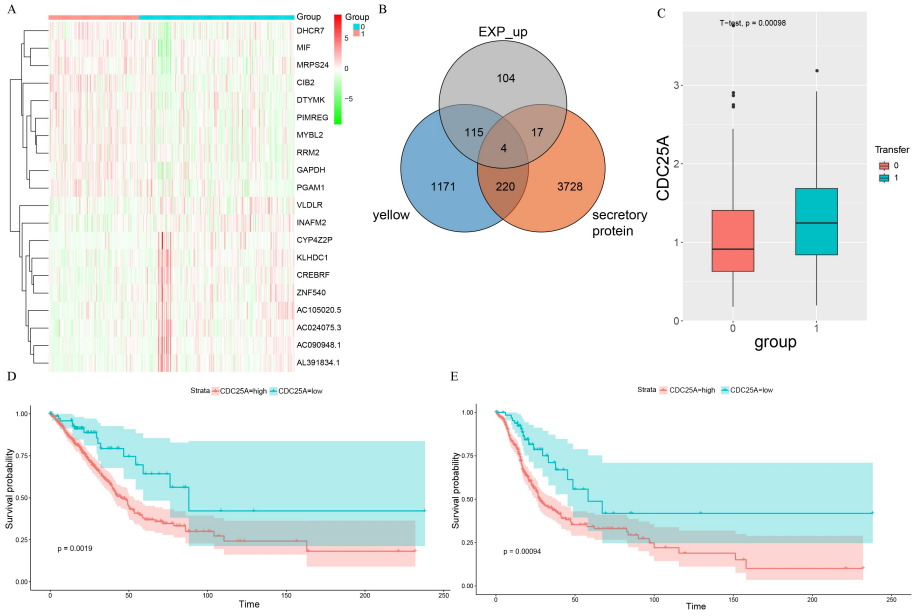

Fig. 3. Identification and analysis of the key candidate gene *CDC25A*. (A) Heatmap showing differentially expressed genes. (B) Venn diagram indicating consensus genes. (C) Box plot representing *CDC25A* expression levels. (D) Overall survival analysis. (E) Disease-free survival analysis.

Results

Identification and Analysis of Key Co-Expression Module.

The mRNA expression profile of 526 patients with LUAD and 59 healthy controls was retrieved from the TCGA database. Patients were divided based on the primary tumor staging (T) according to the TNM classification system. A subset of 320 patients having early-stage tumors (T1 and T2) was identified, where 118 patients exhibited metastasis while 202 patients did not. WGCNA package within R software was applied to this early-stage cohort. By selecting a soft thresholding power of 2 (R^2 = 0.9), a scale-free network topology was established as shown in Fig. 1A,B. The average hierarchical clustering analysis resulted in seven distinct co-expression modules (Fig. 1C). Module-trait correlation analysis revealed that the yellow module exhibited the highest positive correlation with M grade (R = 0.11, p = 0.05), N grade (R = 0.13, p = 0.02), T grade (R = 0.18, p = 0.002) and metastasis status (R = 0.18, p = 0.001), as shown in Fig. 1D. Scatterplot analysis identified a high correlation (cor = 0.55, $p = 4 \times 10^{-120}$) between gene significance (GS) and module membership (MM) (Fig. 1E). By interpreting these initial results, the yellow co-expression module was considered a significant key module associated with early metastasis in LUAD and was selected for further analyses.

Functional Enrichment Analysis of Key Co-Expression Module

GO and KEGG enrichment analyses were performed on key genes in the yellow co-expression module. GO analysis revealed enrichment in several categories, such as chromosomal region (cellular component), nuclear division (biological processes), and DNA catalytic activity (molecular function), as shown in Fig. 2A. KEGG pathway analysis indicated enrichment for the cell cycle pathway (Fig. 2B).

Identification of Key Candidate Genes

Differential gene expression analysis was performed by comparing gene expression profiles of 118 metastatic with 202 non-metastatic early-stage LUAD patients. A heatmap was drawn to visualize the genes with significantly different expressions (Fig. 3A). Overlapping analysis was conducted between 3970 secreted proteins from the HPA, yellow module genes from WGCNA, and genes upregulated in metastatic patients. This analysis identified four candidate genes, including *CDC25A*, cyclin A2 (*CCNA2*), RAD54-like (*RAD54L*), and centromere protein M (*CENPM*) (Fig. 3B). Additionally, the literature review revealed several studies investigating the roles of *CCNA2*, *RAD54L*, and *CENPM* in LUAD [15–17]. However, no study was found regarding the association of *CDC25A* with LUAD. Therefore, the *CDC25A* protein was selected for further analysis. The results from the box plot analysis indicated that *CDC25A* was significantly overexpressed in metastatic patients (Fig. 3C). Furthermore, the early-stage LUAD patients were divided into high and low *CDC25A* expression groups, and overall and disease-free survival

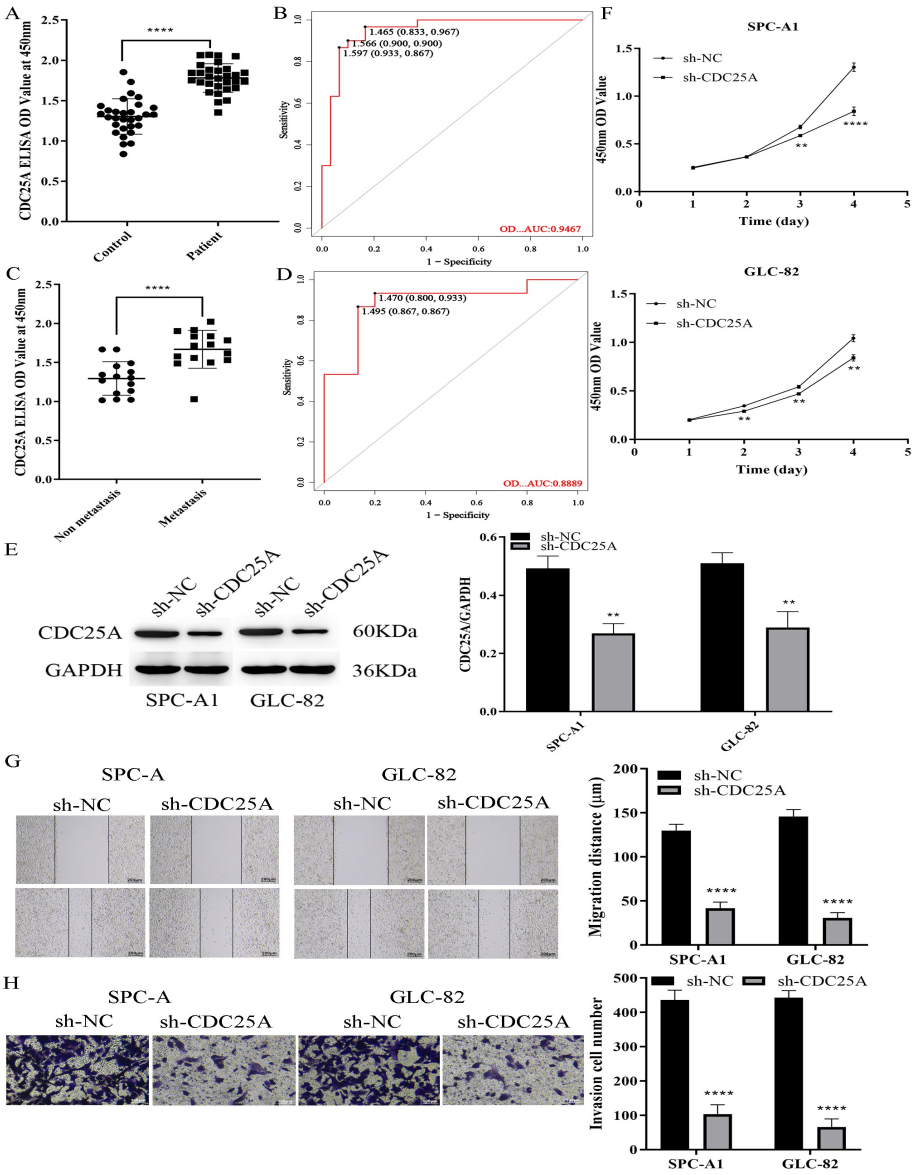

Fig. 4. Analysis of *CDC25A* expression and functional effects of *CDC25A* knockdown. (A,B) Enzyme-linked immunosorbent assay (ELISA) and receiver operating characteristic curve (ROC) curve analysis of *CDC25A* expression levels in early-stage LUAD patients compared to healthy controls (n = 30). (C,D) ELISA and ROC curve analysis of *CDC25A* expression levels in metastatic versus non-metastatic early-stage LUAD patients (n = 15). (E) Western blot (WB) confirmation of *CDC25A* knockdown in lung cancer cells after shRNA transfection (n = 3). (F) Cell Counting Kit-8 (CCK-8) assay of cell proliferation following *CDC25A* knockdown (n = 3). (G) Wound healing assay of cell migration following *CDC25A* knockdown (n = 3). (H) Transwell invasion assay after *CDC25A* knockdown (n = 3). sh-CDC25A, short hairpin RNA targeting CDC25A; sh-NC, negative control sh-RNA; OD, optical density. (**$p < 0.01$, ****$p < 0.0001$).

rates were analyzed. Survival analysis demonstrated improved overall and disease-free survival rate in patients with reduced *CDC25A* expression (Fig. 3D,E).

Elevated CDC25A Expression in Early-Stage LUAD Patients

To validate the overexpression of *CDC25A*, serum samples from 30 early-stage LUAD patients and 30 healthy controls were analyzed using ELISA. We observed that the expression levels of *CDC25A* protein were significantly elevated in LUAD patients compared to healthy controls ($p < 0.0001$, Fig. 4A,B). To investigate the association with metastasis, serum samples from 15 individuals with metastatic early stage LUAD and 15 individuals without metastasis were analyzed. The results from ELISA analysis revealed considerably elevated levels of *CDC25A* expression in metastatic patients ($p < 0.0001$) compared to non-metastatic patients (Fig. 4C,D). These findings collec-

Journal of
BIOLOGICAL REGULATORS
and Homeostatic Agents

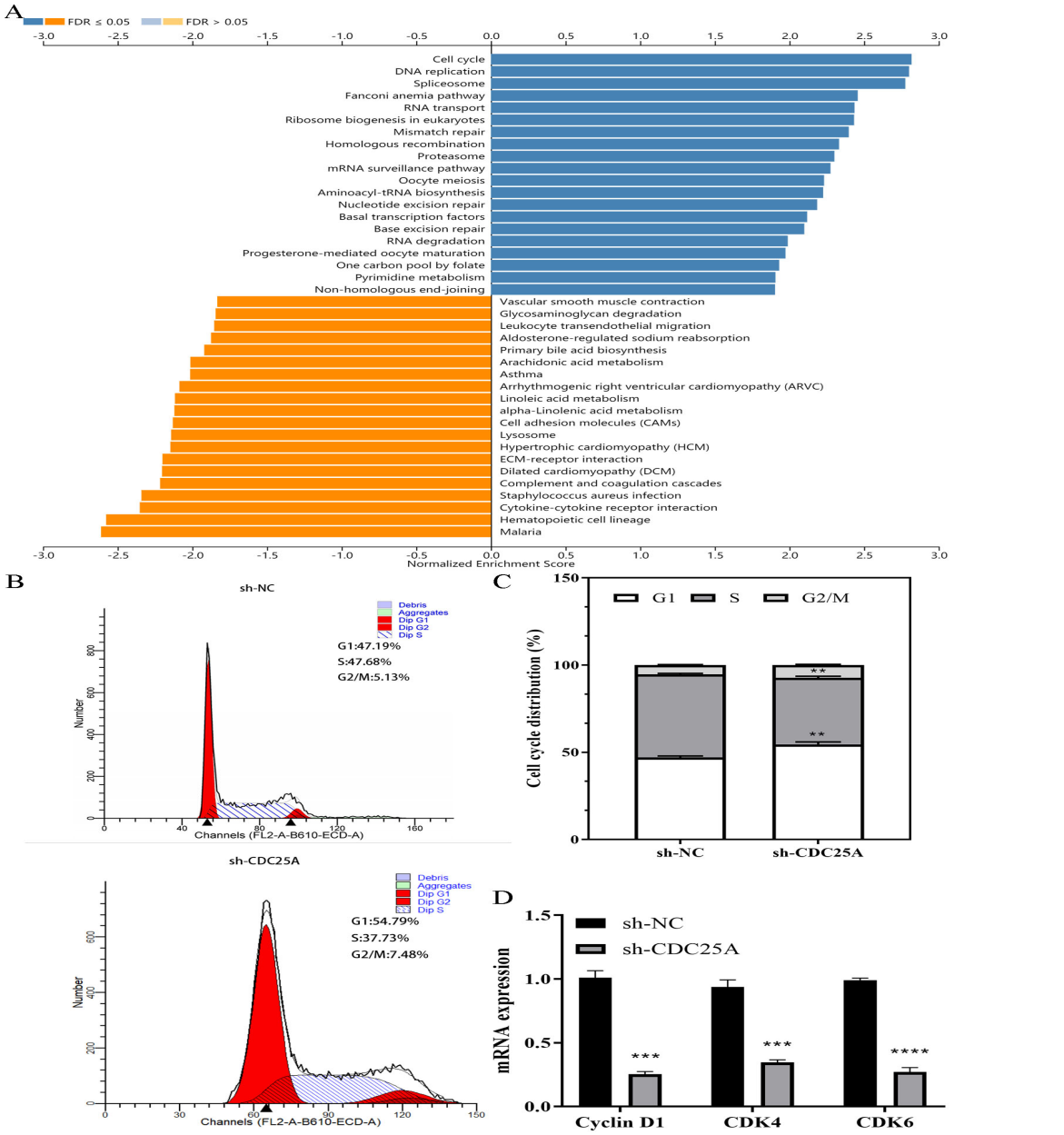

Fig. 5. Pathway analysis for *CDC25A* and its validation in early-stage LUAD metastasis. (A) KEGG pathway analysis of *CDC25A* in early-stage LUAD metastasis. (B) Cell cycle analysis using flow cytometry (n = 3). (C) Quantification of results obtained from flow cytometry (n = 3). (D) qPCR for the expression of *Cyclin D1*, *CDK4* and *CDK6* (n = 3). (**$p < 0.01$, ***$p < 0.001$, ****$p < 0.0001$).

tively confirm that increased *CDC25A* expression is linked to early-stage metastasis in LUAD, thus providing clinical validation.

CDC25A Knockdown Inhibits LUAD Cell Proliferation, Migration, and Invasion

SPC-A1 and GLC-82 LUAD cells were transfected with sh-CDC25A or negative control sh-RNA. The knockdown of *CDC25A* was confirmed using western blot (WB) ($p < 0.01$, Fig. 4E). CCK-8 assay indicated significantly decreased proliferation in cells transfected with sh-CDC25A compared to those transfected with negative control sh-RNA ($p < 0.01$, Fig. 4F). After *CDC25A* knockdown, Wound healing and transwell invasion assay demonstrated a substantial reduction in migration and invasion capabilities, respectively ($p < 0.0001$, Fig. 4G,H). These findings indicate that reducing the expression of *CDC25A* inhibits LUAD cell proliferation, migration, and invasion. These findings, combined with those obtained from computational and clinical analyses, illustrate that overexpression of *CDC25A* is associated with early-stage LUAD metastasis. Therefore, we further hypothesized that expression of the *CDC25A* might be linked with enhanced metastasis in early-stage LUAD.

CDC25A Promotes Cell Cycle Progression in Early-Stage LUAD

To investigate the mechanisms underlying the effect of CDC25A in early-stage LUAD metastasis, 118 patients with metastatic early-stage LUAD were divided into two groups based on *CDC25A* expression levels (high and low expression groups). KEGG pathway analysis revealed enrichment of the cell cycle pathway in the high CDC25A expression group (Fig. 5A). Furthermore, SPC-A1 cells were transfected with sh-CDC25A or negative control sh-RNA and analyzed for cell cycle progression and regulation. The number of cells in each phase was assessed using flow cytometry, and the expression levels of *Cyclin D1*, cyclin-dependent kinase 4 (*CDK4*), and cyclin-dependent kinase 6 (*CDK6*) were determined using qPCR. The results from the flow cytometry revealed that knockdown of *CDC25A* increased the number of cells in the G1 phase while decreasing the number of cells in the S phase compared to negative control sh-RNA ($p < 0.01$, Fig. 5B,C). Additionally, qPCR analysis revealed significantly decreased *Cyclin D1*, *CDK4*, and *CDK6* mRNA levels following *CDC25A* knockdown ($p < 0.001$, Fig. 5D). These findings indicate that *CDC25A* promotes cell cycle progression in early-stage LUAD by regulating the expressions of *Cyclin D1*, *CDK4*, and *CDK6*, and inducing G1/S phase transition.

Discussion

Lung adenocarcinoma (LUAD), a major subtype of non-small cell lung cancer (NSCLC), exhibits a high metastatic potential, contributing to a worse prognosis. Therefore, understanding the regulatory mechanisms underlying LUAD proliferation, invasion, and metastasis is crucial for improving its prognosis and developing potential therapeutics. In this study, we identified key gene modules associated with early LUAD metastasis using WGCNA analysis, revealing that genes within these key modules are prominently associated with cell cycle pathways. Additionally, through differential expression analysis, we identified upregulated genes in the samples with early-stage metastatic LUAD. By integrating these results with secreted protein data from HPA, we observed four proteins, including *CDC25A*, *CCNA2*, *RAD54L*, and *CENPM,* that were overexpressed in both early metastasis and cell cycle-related modules. Previous studies demonstrate that *CCNA2,* in combination with *CDK2*, regulates G1/S transition [18] and exhibits upregulation across several cancers [19]. Overexpression of *RAD54L* is associated with poor prognosis in NSCLC [20–22], whereas *CENPM* promotes LUAD proliferation, invasion, and cell cycle progression [23]. However, the role of *CDC25A* in LUAD remains largely unexplored.

The current study demonstrated that *CDC25A* was overexpressed in patients with metastatic LUAD and associated with a poorer survival rate. Additionally, *CDC25A* was identified to be upregulated in early-stage metastatic LUAD patients. Numerous studies have suggested the role of *CDC25A* in other cancers, including stem cell carcinoma [24], colorectal cancer [25], and cervical cancer [26]. Congruently, our *in vitro* experiments indicated that the knockdown of *CDC25A* inhibits LUAD cell proliferation, migration, and invasion. Furthermore, KEGG pathway analysis of early-stage LUAD patients revealed the correlation between the overexpression of *CDC25A* and cell cycle pathway enrichment.

Cell cycle progression plays a critical role in proliferation. The results from previous studies suggested that *CDK4*, *CDK6*, and *Cyclin D1* were activated during G1/S transition [27,28]. Furthermore, while all three variants of *CDC25* phosphatases regulate mitosis, *CDC25A,* in particular, controls G1-S progression [29,30]. This study also affirmed that *CDC25A* knockdown increases the number of LUAD cells in the G1 phase while decreasing those in the S phase, accompanied by a reduction in *CDK4*, *CDK6*, and *Cyclin D1*. Overall, our results suggest that *CDC25A* promotes LUAD cell cycle progression and proliferation, facilitating the development of LUAD by regulating the cell cycle.

Conclusion

In this study, we identified that overexpression of *CDC25A* in early metastatic LUAD is associated with poor prognosis for patients. Our investigation validated that *CDC25A* knockdown arrests the LUAD cells in the G1 phase, and inhibits their proliferation, migration, and invasion. We identified *CDC25A* as a promoter of early LUAD metastasis through cell cycle regulation. This reveals that *CDC25A* could be a potential prognostic biomarker and therapeutic target for managing early-stage metastatic LUAD. Further research is recommended to investigate the molecular mechanisms responsible for the overexpression of *CDC25A* in metastatic LUAD and its downstream oncogenic effects. Overall, this study provides new insights into the pathogenesis of early LUAD metastasis and suggests *CDC25A* as a significant candidate for the development of targeted therapy.

Abbreviations

LUAD, lung adenocarcinoma; NSCLC, non-small cell carcinoma; CDKs, cyclin-dependent kinases; CDC25, cell division cycle 25; TCGA, The Cancer Genome Atlas; HPA, The Human Protein Atlas; GO, Gene Ontology; KEGG, Kyoto Encyclopedia of Genes and Genomes.

Availability of Data and Materials

The data of this study can be obtained in the TCGA database (https://portal.gdc.cancer.gov/) and HPA (https://www.proteinatlas.org/).

Journal of
BIOLOGICAL REGULATORS
and Homeostatic Agents

Author Contributions

BLi was responsible for the conceptualisation and design of the study. TZ was the administrative support for the study. BLi and XZ were responsible for the design of research. HH and TZ were responsible for the data collection and summarisation. YQ, BLa and BLiu were responsible for data analysis and interpretation. All authors were involved in the writing of the manuscript. The final manuscript was approved by all authors. All authors have participated sufficiently in the work and agreed to be accountable for all aspects of the work.

Ethics Approval and Consent to Participate

The study has been approved by the Second Affiliated Hospital of Qiqihar Medical University Ethical Research Association, and the ethical number is [2021]1215-1. All the study participants provided informed consent.

Acknowledgment

Not applicable.

Funding

This study was supported by the general project of Qiqihar Medical Science Academy (grant numbers QMSI2021M-21) and the research project of Heilongjiang Provincial Health Commission (grant numbers 20220909010622).

Conflict of Interest

The authors declare no conflict of interest.

References

[1] Sher T, Dy GK, Adjei AA. Small cell lung cancer. Mayo Clinic Proceedings. 2008; 83: 355–367.

[2] Hirsch FR, Scagliotti GV, Mulshine JL, Kwon R, Curran WJ, Jr, Wu YL, *et al*. Lung cancer: current therapies and new targeted treatments. Lancet (London, England). 2017; 389: 299–311.

[3] Siegel RL, Miller KD, Jemal A. Cancer statistics, 2018. CA: a Cancer Journal for Clinicians. 2018; 68: 7–30.

[4] Goldstraw P, Chansky K, Crowley J, Rami-Porta R, Asamura H, Eberhardt WEE, *et al*. The IASLC Lung Cancer Staging Project: Proposals for Revision of the TNM Stage Groupings in the Forthcoming (Eighth) Edition of the TNM Classification for Lung Cancer. Journal of Thoracic Oncology: Official Publication of the International Association for the Study of Lung Cancer. 2016; 11: 39–51.

[5] Walters S, Maringe C, Coleman MP, Peake MD, Butler J, Young N, *et al*. Lung cancer survival and stage at diagnosis in Australia, Canada, Denmark, Norway, Sweden and the UK: a population-based study, 2004-2007. Thorax. 2013; 68: 551–564.

[6] Golias CH, Charalabopoulos A, Charalabopoulos K. Cell proliferation and cell cycle control: a mini review. International Journal of Clinical Practice. 2004; 58: 1134–1141.

[7] Vermeulen K, Van Bockstaele DR, Berneman ZN. The cell cycle: a review of regulation, deregulation and therapeutic targets in cancer. Cell Proliferation. 2003; 36: 131–149.

[8] Malumbres M, Barbacid M. To cycle or not to cycle: a critical decision in cancer. Nature Reviews Cancer. 2001; 1: 222–231.

[9] Ekholm SV, Reed SI. Regulation of G(1) cyclin-dependent kinases in the mammalian cell cycle. Current Opinion in Cell Biology. 2000; 12: 676–684.

[10] Sur S, Agrawal DK. Phosphatases and kinases regulating CDC25 activity in the cell cycle: clinical implications of CDC25 overexpression and potential treatment strategies. Molecular and Cellular Biochemistry. 2016; 416: 33–46.

[11] Cangi MG, Cukor B, Soung P, Signoretti S, Moreira G, Jr, Ranashinge M, *et al*. Role of the Cdc25A phosphatase in human breast cancer. The Journal of Clinical Investigation. 2000; 106: 753–761.

[12] Ding FN, Gao BH, Wu X, Gong CW, Wang WQ, Zhang SM. miR-122-5p modulates the radiosensitivity of cervical cancer cells by regulating cell division cycle 25A (CDC25A). FEBS Open Bio. 2019; 9: 1869–1879.

[13] Wang B, Gong Q, Chen F. CDC25A inhibition suppresses cell proliferation and induces G_1/S phase cell cycle arrest in nasopharyngeal carcinoma. Molecular Medicine Reports. 2023; 27: 109.

[14] Lin TC, Lin PL, Cheng YW, Wu TC, Chou MC, Chen CY, *et al*. MicroRNA-184 Deregulated by the MicroRNA-21 Promotes Tumor Malignancy and Poor Outcomes in Non-small Cell Lung Cancer via Targeting CDC25A and c-Myc. Annals of Surgical Oncology. 2015; 22 Suppl 3: S1532–S1539.

[15] Li Z, Zhang Y, Zhou Y, Wang F, Yin C, Ding L, *et al*. Tanshinone IIA suppresses the progression of lung adenocarcinoma through regulating CCNA2-CDK2 complex and AURKA/PLK1 pathway. Scientific Reports. 2021; 11: 23681.

[16] Zheng S, Yao L, Li F, Huang L, Yu Y, Lin Z, *et al*. Homologous recombination repair rathway and RAD54L in early-stage lung adenocarcinoma. PeerJ. 2021; 9: e10680.

[17] Liu C, Wang Y, Dao Y, Wang S, Hou F, Yang Z, *et al*. Upregulation of CENPM facilitates lung adenocarcinoma progression via PI3K/AKT/mTOR signaling pathway. Acta Biochimica et Biophysica Sinica. 2022; 54: 99–112.

[18] Wu J, Lv Q, He J, Zhang H, Mei X, Cui K, *et al*. MicroRNA-188 suppresses G1/S transition by targeting multiple cyclin/CDK complexes. Cell Communication and Signaling: CCS. 2014; 12: 66.

[19] Li JA, Liu BC, Song Y, Chen X. Cyclin A2 regulates symmetrical mitotic spindle formation and centrosome amplification in human colon cancer cells. American Journal of Translational Research. 2018; 10: 2669–2676.

[20] Qiao GB, Wu YL, Yang XN, Zhong WZ, Xie D, Guan XY, *et al*. High-level expression of Rad51 is an independent prognostic marker of survival in non-small-cell lung cancer patients. British Journal of Cancer. 2005; 93: 137–143.

[21] Liu YB, Mei Y, Tian ZW, Long J, Luo CH, Zhou HH. Down-regulation of RIF1 Enhances Sensitivity to Platinum-Based Chemotherapy in Epithelial Ovarian Cancer (EOC) by Regulating Nucleotide Excision Repair (NER) Pathway. Cellular Physiology and Biochemistry: International Journal of Experimental Cellular Physiology, Biochemistry, and Pharmacology. 2018; 46: 1971–1984.

[22] Mazin AV, Mazina OM, Bugreev DV, Rossi MJ. Rad54, the motor of homologous recombination. DNA Repair. 2010; 9: 286–302.

[23] Qi N, Niu Y, Li Z, Xiao L, Tang D, Gao W. The prognostic value and mechanisms of centromere protein M in patients with lung adenocarcinoma. Translational Cancer Research. 2022; 11: 3471–3490.

[24] Xu X, Yamamoto H, Sakon M, Yasui M, Ngan CY, Fukunaga H, *et al*. Overexpression of CDC25A phosphatase is associated

with hypergrowth activity and poor prognosis of human hepatocellular carcinomas. Clinical Cancer Research: an Official Journal of the American Association for Cancer Research. 2003; 9: 1764–1772.

[25] Guo P, Zu S, Han S, Yu W, Xue G, Lu X, *et al*. BPTF inhibition antagonizes colorectal cancer progression by transcriptionally inactivating Cdc25A. Redox Biology. 2022; 55: 102418.

[26] Qi J, Zhou L, Li D, Yang J, Wang H, Cao H, *et al*. Oncogenic role of ALX3 in cervical cancer cells through KDM2B-mediated histone demethylation of CDC25A. BMC Cancer. 2021; 21: 819.

[27] Sherr CJ. The Pezcoller lecture: cancer cell cycles revisited. Cancer Research. 2000; 60: 3689–3695.

[28] Sage J. Cyclin C makes an entry into the cell cycle. Developmental Cell. 2004; 6: 607–608.

[29] Jinno S, Suto K, Nagata A, Igarashi M, Kanaoka Y, Nojima H, *et al*. Cdc25A is a novel phosphatase functioning early in the cell cycle. The EMBO Journal. 1994; 13: 1549–1556.

[30] Blomberg I, Hoffmann I. Ectopic expression of Cdc25A accelerates the G(1)/S transition and leads to premature activation of cyclin E- and cyclin A-dependent kinases. Molecular and Cellular Biology. 1999; 19: 6183–6194.